Algorithms and Bounds for Estimating Location, Directionality, and Environmental Parameters of Primary Spectrum Users

Richard K. Martin, *Member, IEEE*, and Ryan Thomas, *Member, IEEE*

***Abstract*—Most existing work on dynamic spectrum access deals with creating a spectral and temporal map of spectrum white space, and then filling it. The spectrum can be better utilized by increasing the spatial awareness of secondary users to include knowledge of the locations of all primary and secondary users, as well as the orientations and parameters of their directional or omni-directional antennas. This paper derives a Maximum Likelihood (ML) algorithm, an approximate ML algorithm, and associated performance bounds for jointly estimating a transmitter's position, orientation, beam width, and transmit power, as well as the environment's path loss exponent, using received signal strength measurements. The methods can be used for either a primary or secondary user. Simulations are used to determine what types of sensor geometries lead to good estimates of each parameter, to evaluate the performance of the estimators, and to determine spectrum availability as a function of spatial coordinates.**

***Index Terms*—Cognitive networks, Cramer-Rao lower bounds, dynamic spectrum access, received signal strength, sensor networks.**

I. Introduction

THE Cognitive Radio (CR) concept shows great promise in providing intelligent multifunction, multi-domain communication devices. Particularly for the Dynamic Spectrum Access (DSA) problem of allowing the re-use of spectrum allocated to primary users (users with primary license to a frequency band) by secondary users (users without a full license or priority in a frequency band), CRs are a potentially powerful solution. However, CRs are not suited to accomplishing *network* objectives due to their limited, localized viewpoint of the Radio Frequency (RF) environment. Their focus on optimizing local radio parameters may come at the expense of users of the RF environment that are participating in achieving the same network objectives. This can directly degrade the network's multi-hop performance by compromising the available bandwidth and signal-to-noise ratio on links of the network topology.

Manuscript received April 8, 2009; revised July 6, 2009 and September 29, 2009; accepted October 2, 2009. The associate editor coordinating the review of this paper and approving it for publication was G. Colavolpe.

R. Martin (corresponding author) and R. Thomas are with the Dept. of Electrical and Computer Engineering, The Air Force Inst. of Technology (AFIT), Wright-Patterson AFB, OH (e-mail: {richard.martin, ryan.thomas}@afit.edu).

R. Martin and R. Thomas are funded in part by the Air Force Research Labs, Sensors Directorate. The views expressed in this paper are those of the authors, and do not reflect the official policy or position of the United States Air Force, Department of Defense, or the U.S. Government. This document has been approved for public release; distribution unlimited.

Digital Object Identifier 10.1109/TWC.2009.090494

The concept of a Cognitive Radio Network (CRN) rather than individual CRs is just beginning to receive attention; perhaps the first serious investigation occurred in [1], where the features, objectives, and challenges of Cognitive Networks (CNs) (a superset of the CRN concept) were investigated. In this paper, CNs, and by extension CRNs, are distinguished from CRs by their end-to-end focus. Currently, most research in the field focuses on CRN architectures for problems in the mobility or DSA fields [2], [3]. Very little work has been done on the foundational underpinnings of the CRN. Particularly to achieve DSA objectives in a network environment, each CR in the CRN needs a shared network-level view of the RF environment.

Towards this end, recent advances have been made determining the presence or absence of primary users in the RF environment. By cooperatively sharing local estimates on the presence of primary users, [4] and [5] have shown the accuracy of these detection algorithms can be increased. However, simply knowing whether or not there exists a user in a particular frequency band is not enough information. To make network-wide decisions that do not mis-estimate the RF impact of a source, estimates of the spatial positioning and antenna gain are also needed. When location and gain pattern estimation are combined with signal classification and identification estimates, the resulting "map" of spectrum usage in space, time, frequency, and code forms what we call a "5.1 dimensional RF topography," with the "5" representing the five dimensions of time, frequency, and space, and the ".1" representing additional supplementary information such as modulation classification or under-use of available spreading codes. An example of the topography estimation process by a network of radios is visually illustrated in Fig. 1. A diverse range of future CRN applications can use this topography to perform such tasks as determining spectral-aware waveforms for network communication; locating and observing other radio entities (primary or secondary users) in the region; spectrum policing; and creating efficient connection topologies.

The 5.1 dimensional RF topography is similar to the Radio Environment Map (REM) proposed in [6]. The REM is a comprehensive multi-dimensional "map" that identifies the location and geo-spatial properties of parameters such as terrain, service availability, policy requirements, and hardware type. However, the REM is envisioned as a centralized, *a priori* database that is disseminated throughout the network and occasionally updated or corrected, rather than created in a distributed, near-real time fashion. The RF topography

1536-1276/09$25.00 © 2009 IEEE

may fit into the REM as an Available Resource Map (ARM), which the authors describe as a a real time map of all radio activity in the network. An RF topography scheme created by RSS should be a significant improvement previous ARM proposals [7], which required specializing positioning sensors (such as GPS) and self-reporting by the transmitters of their RF characteristics.

Spatial estimation of the location of signal sources, or "source localization," is currently an active area of research, with many interesting non-CN applications. For example, precision location of cell phones in an emergency has been mandated in the United States [8]. Similarly, microphone arrays can be used to determine the location of an acoustic source [9], to aid automatic camera tracking [10] or determination of the source of sniper fire [11].

Measurements that can be taken to aid source localization include the Angle of Arrival (AOA) [12], the Received Signal Strength (RSS) [9], [13], or the Time Difference of Arrival (TDOA) at multiple receivers [14]. The drawbacks of AOA measurements are that the quality of the final position estimate degrades rapidly as the receivers move away from the source, and that determining the AOA requires a phased array of antennae at each sensor rather than a single antenna. RSS is frequently used due to its simplicity, despite the fact that RSS measurements are not very accurate and a large, dense sensor network is often required for precise location estimates. RSS techniques typically assume that the transmitted power and the path loss exponent are known (or are sometimes included as additional parameters to be estimated [15]), that there is no multipath or shadowing, and that the transmitter is isotropic. TDOA methods do not make such assumptions, but they require significantly higher communications overhead than AOA or RSS. We focus on RSS in this paper, although RSS can be combined with TDOA measurements to improve the accuracy of the estimator [16].

One major drawback of most existing work is the assumption of isotropic (omni-directional) transmission. Since most modern communications devices exploit spatial diversity through non-uniform antenna gain patterns, the isotropic assumption is rarely valid. Cell phone handsets, for example, attempt to direct radiation away from the head, resulting in shadowing on one side of the phone; and base stations generally employ phased arrays of antennas to shape the transmit gain pattern. Knowing the direction in which a transmitter is transmitting can allow for more efficient use of spectrum. This paper removes the isotropic assumption and considers estimation of the directionality, position, and parameters of an RF transmission via a sensor network. Note that if there are many scatterers close to the transmitter, it will blur the effects of the radiation pattern; however, we assume that a variable beam width is to be estimated, which helps account for such possible blurring. Moreover, scatterers close to the sensors will have roughly the same angle to the transmitter as the sensors, and will not be a problem. The fact that the transmitter is using a directional antenna presupposes that it is in an environment in which the effects of directionality would be completely obscured.

To determine bounds on the variances of the parameter estimates, we will use the Cramer-Rao Lower Bound (CRLB) [17]. The CRLB is is a bound on the covariance matrix of unbiased estimates of the parameter vector $\mathbf{z}$, where $\mathbf{z}$ contains parameters such as the spatial location (x_0, y_0), beam orientation (θ_0), beam half-width (σ_N), transmission power (P_0), or path-loss exponent (n_p). In particular, the diagonal elements of the CRLB bound the variances of unbiased estimates of the corresponding scalar parameters. By computing the CRLB, we determine the lowest possible estimation variance we can achieve, regardless of which algorithm or method is used in the estimation process. A variance equal to the CRLB is not necessarily achievable, but in practice it is usually possible to get very close to the bound with some estimator. By computing the CRLB for various sensor geometries, we will determine which possible arrangements of sensors will potentially lead to good estimates (i.e. low variance) of the source position, orientation, and environmental parameters. Better estimates of these parameters will allow us to better estimate the power incident at any point in the RF topography, whether we have a sensor there or not.

There is a large amount of existing work on localization using RSS measurements, although for the case of omni-directional antennas. In [18], a CRLB was derived for estimates of the source 2D coordinates and (omni-directional) transmit power using RSS measurements. Similarly, in [19], the CRLB and a Maximum Likelihood (ML) estimator were derived under the same conditions for self-localization of a network of sensors, in which a small subset of the sensors were "anchor nodes" at known locations. In [20], the Barankin bound was computed under the same assumptions. It was shown that the Barankin bound is tighter than the CRLB, although it is more difficult to compute. In [15], the estimation problem was expanded to include the path loss exponent (as suggested in [19]), although the estimator was not an ML estimator and analytical performance bounds were not considered.

In Section II, we present the system model, including both a Gaussian-shaped radiation pattern and a more general model. In Section III, we derive analytic expressions for the CRLBs on estimates of the source position, orientation, beam half-width, power, and path loss exponent, for the Gaussian-shaped pattern. The derivation extends to the general case, but is not very interesting without assuming a specific functional form. In Section IV, we derive an ML estimation algorithm for the unknown parameters, as well as an approximately ML algorithm with significantly reduced complexity, for both the Gaussian and general radiation patterns. Section V provides examples of numerical evaluation of the bounds and estimator performance for various sensor configurations, and Section VI concludes the paper.

II. System Model

Throughout, $(\cdot)^*$, $(\cdot)^T$, $(\cdot)^H$, and $\mathcal{E}\{\cdot\}$ denote complex conjugate, matrix transpose, conjugate (Hermitian) transpose, and statistical expectation, respectively. A sample average is denoted $\langle\cdot\rangle$, i.e. sum up the arguments and divide by their cardinality. The matrices $\mathbf{0}$, $\mathbf{1}$ contain all zeros or all ones respectively, and when it is not clear from the context, they will be subscripted with their dimensionality. A hat indicates an estimate of its argument, e.g. $\widehat{\theta_0}$ is an estimate of θ_0.

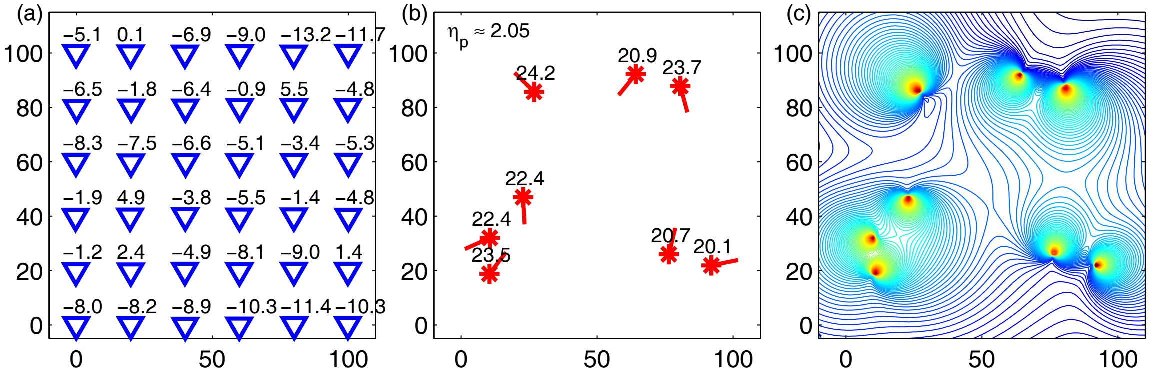

Fig. 1. Creation of a 5.1D RF topography, to find *spatial* spectrum white space. (a) First, power levels are observed at each sensor ▽. (b) Next, the source locations ∗, transmitted power levels, antenna orientations, antenna beam widths (not shown), and path loss exponent are estimated. (c) Finally, a topographical map is created of (estimated) power incident on *any* point in space, not just points where there are sensors.

Directionality in transmissions can be created using a phased array or via a single directional antenna, although we focus on the latter case for simplicity. Consider a directional antenna with a Gaussian-shaped radiation pattern,

$$|G_N(\theta)|^2 = \Gamma_0 \exp\left(\frac{-(\mathcal{M}(\theta-\theta_0))^2}{2\sigma_N^2}\right), \tag{1}$$

where the antenna is located at (x_0, y_0) with the main beam in the direction θ_0, Γ_0 is chosen to scale the transmitted power, and the function $\mathcal{M}(\cdot)$ restricts the argument to $[-\pi, \pi]$ via

$$\mathcal{M}(\phi) = \mathrm{mod}_{2\pi}(\phi+\pi) - \pi. \tag{2}$$

Note that the term "Gaussian" here simply refers to the bell curve shape of the radiation pattern, not to a random variable.

The Gaussian shape could be used to approximate the main lobe of a more generic radiation pattern (such as from a phased array). For the sake of generality, we also explicitly consider a generic radiation pattern, written as

$$10\log_{10}|G_g(\theta)|^2 = 10\log_{10}\Gamma_0 - \gamma(\mathcal{M}(\theta-\theta_0)), \tag{3}$$

where γ can be any function that satisfies both $\gamma(0) = 0$ and $\gamma(u) \geq 0\ \forall u$. As before, Γ_0 scales the peak power. Equation (1) is produced, for example, if $\gamma(u) = \left(u^2/\sigma_N^2\right)\ 5\log_{10} e$. For the sake of gaining intuition as to the functional dependence of the CRLB on the various parameters, we will usually use (1) rather than (3) in our derivations; however, the ML estimation algorithms in Section IV will consider both the specific and general cases.

The S CR nodes (the sensors) are located at known positions (x_s, y_s), for $s = 1, 2, \cdots, S$, thus they are at distances and angles

$$d_s = \sqrt{(x_s - x_0)^2 + (y_s - y_0)^2}, \tag{4}$$

$$\theta_s = \arctan\left(\frac{y_s - y_0}{x_s - x_0}\right), \tag{5}$$

with respect to the source.

Assuming log-normal fading as in [15], [18], the received power in the dB domain at each sensor is normally distributed with variance σ^2, as per the Okumura-Hata model [21]. Typically, σ ranges from 4 dB to 12 dB [22], corresponding to uncluttered environments (e.g. deserts) to environments rich in shadowing and multipath (e.g. urban canyons). The value of σ^2 is usually approximated from controlled measurements in a given environment; but it could be considered a quantity to be estimated as well. In free space, power diminishes according to an inverse square law, but due to multipath and shadowing the path loss exponent n_p need not be 2. Typically, $n_p \approx 2$ in free space propagation and $n_p \approx 5$ in dense urban environments [18], though some sources state that typical values of n_p are in the range 2 to 4. Since it is typical to work in the log domain, we also define P_0 as the dB version of Γ_0. Thus, altogether, our potential unknowns for a single directional antenna are x_0, y_0, θ_0, P_0, n_p, and σ_N, though some may be known *a priori*.

In the log domain, the received power is Gaussian, modelled as

$$\mathbf{p} = [p_1, \cdots, p_S]^T \sim \mathcal{N}(\mathbf{m}, \mathbf{C}), \tag{6}$$

using the definitions

$$\mathbf{m} = [m_1, \cdots, m_S]^T, \tag{7}$$

$$\begin{aligned} m_s &= 10\log_{10}\left(|G(\theta_s)|^2\right) - n_p 10\log_{10}\left(\frac{d_s}{d_0}\right), \\ &= P_0 - \frac{b}{2}(\mathcal{M}(\theta_s - \theta_0))^2 - n_p \overline{d}_s, \end{aligned} \tag{8}$$

$$P_0 = 10\log_{10}(\Gamma_0), \tag{9}$$

$$b = \frac{10\log_{10}(e)}{\sigma_N^2}, \tag{10}$$

$$\overline{d}_s = 10\log_{10}(d_s/d_0) \tag{11}$$

where the parameter d_0 is a short reference distance from the receiver (typically 1 m). In most of our simulations, we assume $\mathbf{C} = \sigma^2\mathbf{I}$, which covers most cases of practical interest, but the derivations are left in the general case whenever it is easy to do so.

For the CRLB calculations and derivation of the ML estimator, it is useful to explicitly state the log of the Probability Density Function (PDF) associated with (6), known as the log-likelihood:

$$\begin{aligned} L &= \ln f(\mathbf{p}|\mathbf{z}) \\ &= -\frac{1}{2}(\mathbf{p}-\mathbf{m})^T \mathbf{C}^{-1}(\mathbf{p}-\mathbf{m}), \end{aligned} \tag{12}$$

ignoring a constant term that will cancel due to differentiation.

III. Performance Bounds

In this section, we derive CRLBs on the variances of unbiased estimates of the various transmission parameters, given the RSS at a collection of sensors at known locations. These include transmitter location, transmitter orientation, transmit power, the path loss exponent, and the beam half-width. We first derive the general results, and then consider two special cases in order to simplify the results and gain some intuition.

In its simplest form, the CRLB is a bound on unbiased estimates of non-random parameters (or parameters whose probability distributions are not known *a priori*) [17]. Specifically, the covariance of unbiased estimates of the M unknowns grouped into the vector $\mathbf{z}$ is lower-bounded (in the matrix sense) by $\mathbf{J}^{-1}$, where the Fisher Information Matrix (FIM) $\mathbf{J}$ is defined by:

$$J_{i,j} = -\mathcal{E}\left\{\frac{\partial^2 L}{\partial z_i \partial z_j}\right\}, \tag{13}$$

where L is the log-likelihood given by (12). In particular, the variances of the estimates of elements of $\mathbf{z}$ are bounded by the diagonal of $\mathbf{J}^{-1}$. In the remainder of this section, we derive the CRLB for the probability density given in Section II.

A. All six parameters unknown

The log-likelihood of the RSS vector $\mathbf{p}$ given the vector of unknowns $\mathbf{z}$ is given by (12). The vector $\mathbf{z}$ contains some or all of P_0 (or Γ_0), b (or σ_N), n_p, x_0, y_0, and θ_0, depending on which parameters are already known. For the Gaussian case of (12), the FIM simplifies to

$$\begin{aligned} J_{i,j} &= \mathcal{E}\left\{\frac{\partial}{\partial z_i}\left[(\mathbf{p}-\mathbf{m})^T \mathbf{C}^{-1}\frac{\partial}{\partial z_j}(\mathbf{p}-\mathbf{m})\right]\right\} \\ &= \left(\frac{\partial}{\partial z_i}\mathbf{m}\right)^T \mathbf{C}^{-1}\frac{\partial}{\partial z_j}\mathbf{m} \end{aligned} \tag{14}$$

since $\mathcal{E}\{\mathbf{p}\} = \mathbf{m}$. For i.i.d. noise, (14) could further simplify to

$$J_{i,j} = \frac{1}{\sigma^2}\left(\frac{\partial}{\partial z_i}\mathbf{m}\right)^T \frac{\partial}{\partial z_j}\mathbf{m}. \tag{15}$$

Depending on which parameters are assumed unknown, the relevant partial derivatives are given by a subset of

$$\frac{\partial m_s}{\partial P_0} = 1 \tag{16}$$

$$\frac{\partial m_s}{\partial b} = \frac{-1}{2}\left(\mathcal{M}(\theta_s - \theta_0)\right)^2 \tag{17}$$

$$\frac{\partial m_s}{\partial n_p} = -\overline{d}_s \tag{18}$$

$$\frac{\partial m_s}{\partial \theta_0} = b\ \mathcal{M}(\theta_s - \theta_0) \tag{19}$$

$$\frac{\partial m_s}{\partial x_0} = \frac{-b}{d_s^2}\mathcal{M}(\theta_s - \theta_0)(y_s - y_0) + \frac{10 n_p}{d_s^2}(x_s - x_0) \tag{20}$$

$$\frac{\partial m_s}{\partial y_0} = \frac{-b}{d_s^2}\mathcal{M}(\theta_s - \theta_0)(x_s - x_0) + \frac{10 n_p}{d_s^2}(y_s - y_0) \tag{21}$$

which used the fact that $\frac{\partial \mathcal{M}(\phi)}{\partial \phi} = 1$ (ignoring the single point of discontinuity in the mod function). To cast the bounds for P_0 and b into the form of bounds for Γ_0 and σ_N, we use the CRLB of functions of parameters [17, p.229], given in this case by

$$\begin{aligned} VAR\left\{\widehat{\Gamma_0}\right\} &\geq \left(\frac{\partial \Gamma_0}{\partial P_0}\right)^2 VAR\left\{\widehat{P_0}\right\} \\ &\geq \left(\frac{\Gamma_0 \ln(10)}{10}\right)^2 VAR\left\{\widehat{P_0}\right\}, \end{aligned} \tag{22}$$

$$\begin{aligned} VAR\{\widehat{\sigma_N}\} &\geq \left(\frac{\partial \sigma_N}{\partial b}\right)^2 VAR\left\{\hat{b}\right\} \\ &\geq \left(\frac{\sigma_N^3}{20\log_{10}(e)}\right)^2 VAR\left\{\hat{b}\right\}. \end{aligned} \tag{23}$$

Note that the results in this subsection are a generalization of those in [18]. Specifically, [18] assumed n_p was known and implicitly used the model $b = 0$ (i.e. $\sigma_N = \infty$), hence the b, n_p, and θ_0 terms were not included in the FIM, making it 3×3 rather than 6×6. Moreover, $b = 0$ causes the first term in (20) and (21) to drop out, further simplifying the FIM in [18].

In principle, we can now numerically evaluate the CRLB on Γ_0, σ_N, n_p, x_0, y_0, and θ_0. However, the full 6×6 FIM cannot be (concisely) inverted in closed form, so in order to gain some intuition, we now consider two special cases that allow the FIM to simplify somewhat.

B. Known location and beam width

Assume the source coordinates (x_0, y_0) and the beam half-width σ_N are known, so that $\mathbf{z} = [P_0, n_p, \theta_0]^T$. In most work on source localization, the source coordinates are considered the key parameters to be determined, hence it may seem odd to assume they are known. However, what distinguishes this paper is the estimation of the source's RF footprint, rather than simply its location. The coordinates may be available from a TDOA method, or in the case where the primary user's location is fixed but the angle of transmission is not (e.g. cell phone towers), or possibly by cooperation from the primary user itself. Moreover, even if this assumption does not hold, the simplified mathematical expressions derived in this section may be used to gain some intuition even in the more general case. We will also make the simplifying assumption $\mathbf{C} = \sigma^2\mathbf{I}$ (which holds true in most practical cases), and we adopt the shorthand

$$\mathcal{M}^n \triangleq \left(\mathcal{M}(\theta_s - \theta_0)\right)^n \tag{24}$$

to condense some of the bulkier equations.

Using (15)–(21), the FIM is given by

$$\mathbf{J} = \frac{S}{\sigma^2}\begin{bmatrix} 1 & -\langle \overline{d}_s \rangle & b\langle \mathcal{M} \rangle \\ -\langle \overline{d}_s \rangle & \langle \overline{d}_s^2 \rangle & -b\langle \mathcal{M}\ \overline{d}_s \rangle \\ b\langle \mathcal{M} \rangle & -b\langle \mathcal{M}\ \overline{d}_s \rangle & b^2\langle \mathcal{M}^2 \rangle \end{bmatrix} \tag{25}$$

Recall that the notation $\langle\cdot\rangle$ means "sample average." To gain some intuition, assume the sensors are distributed roughly symmetrically with respect to the direction of transmission, so that $\langle(\mathcal{M}(\theta_s - \theta_0))\rangle \approx 0$ and $\langle(\mathcal{M}(\theta_s - \theta_0))\,\overline{d}_s\rangle \approx 0$. This need not require the sensors to all be on the same radius. This situation could occur, for example, in a very dense sensor network surrounding the source; and other examples are given in Section V. Then

$$\mathbf{J} \approx \frac{S}{\sigma^2}\begin{bmatrix} 1 & -\langle \overline{d}_s \rangle & 0 \\ -\langle \overline{d}_s \rangle & \left\langle \overline{d}_s^2 \right\rangle & 0 \\ 0 & 0 & b^2\left\langle \left(\mathcal{M}\left(\theta_s-\theta_0\right)\right)^2\right\rangle \end{bmatrix}, \quad (26)$$

which is a block matrix and can be block-inverted. Performing the block inverse and using (22),

$$VAR\left\{\widehat{P_0}\right\} \geq \frac{\sigma^2}{S}\frac{\left\langle \overline{d}_s^2\right\rangle}{\left\langle \overline{d}_s^2\right\rangle - \langle \overline{d}_s\rangle^2} \quad (27)$$

$$VAR\left\{\widehat{\Gamma_0}\right\} \geq \left(\frac{\Gamma_0 \ln(10)}{10}\right)^2 \frac{\sigma^2}{S}\frac{\left\langle \overline{d}_s^2\right\rangle}{\left\langle \overline{d}_s^2\right\rangle - \langle \overline{d}_s\rangle^2} \quad (28)$$

$$VAR\left\{\widehat{n_p}\right\} \geq \frac{\sigma^2}{S}\frac{1}{\left\langle \overline{d}_s^2\right\rangle - \langle \overline{d}_s\rangle^2} \quad (29)$$

$$VAR\left\{\widehat{\theta_0}\right\} \geq \frac{\sigma^2}{S}\left(\frac{\sigma_N^2}{10\log_{10}(e)}\right)^2 \frac{1}{\left\langle \left(\mathcal{M}\left(\theta_s-\theta_0\right)\right)^2\right\rangle} \quad (30)$$

Note that since $\langle \theta_s \rangle \approx \theta_0$, the denominator terms are the sample variances of the distances (in dB) and the angles, measured with respect to the transmitter position and orientation.

The transmitter's antenna beam width σ_N and the measurement noise variance σ^2 are beyond our control. The CRLB can be reduced linearly for all three unknowns by increasing the number of sensors S. The variances of estimates of the path loss exponent n_p and the orientation θ_0 can be reduced by increasing the dispersion of the sensors in distance and angle, respectively. The variance of the estimate of the transmit power can be reduced by increasing the dispersion of the sensors in distance with respect to their second moment, or equivalently by holding the mean distance (in dB) constant while increasing the dispersion. In Section V, the CRLB will be numerically computed for different sensor geometries, to show that this intuition still holds when all six parameters are unknown.

C. Known location and path loss

Now assume the source coordinates (x_0, y_0) and the path loss exponent n_p are known, so that $\mathbf{z} = [P_0, b, \theta_0]^T$. As before, the coordinates may be available from a TDOA method; and the path loss exponent may be measured in advance for a given environment. Again, $\mathbf{C} = \sigma^2\mathbf{I}$.

Using (15)–(21), the FIM is given by

$$\mathbf{J} = \frac{S}{\sigma^2}\begin{bmatrix} 1 & \frac{-1}{2}\langle \mathcal{M}^2\rangle & b\langle \mathcal{M}\rangle \\ \frac{-1}{2}\langle \mathcal{M}^2\rangle & \frac{1}{4}\langle \mathcal{M}^4\rangle & \frac{-b}{2}\langle \mathcal{M}^3\rangle \\ b\langle \mathcal{M}\rangle & \frac{-b}{2}\langle \mathcal{M}^3\rangle & b^2\langle \mathcal{M}^2\rangle \end{bmatrix} \quad (31)$$

To gain some intuition, again assume the sensors are distributed roughly symmetrically with respect to the direction of transmission, so that $\langle \mathcal{M}\left(\theta_s-\theta_0\right)\rangle \approx 0$ and $\left\langle \left(\mathcal{M}\left(\theta_s-\theta_0\right)\right)^3\right\rangle \approx 0$. Then

$$\mathbf{J} \approx \frac{S}{\sigma^2}\begin{bmatrix} 1 & \frac{-1}{2}\langle \mathcal{M}^2\rangle & 0 \\ \frac{-1}{2}\langle \mathcal{M}^2\rangle & \frac{1}{4}\langle \mathcal{M}^4\rangle & 0 \\ 0 & 0 & b^2\langle \mathcal{M}^2\rangle \end{bmatrix}, \quad (32)$$

which is a block matrix and can be block-inverted. Performing the block inverse and using (22) and (23),

$$VAR\left\{\widehat{P_0}\right\} \geq \frac{\sigma^2}{S}\frac{\langle \mathcal{M}^4\rangle}{\langle \mathcal{M}^4\rangle - \langle \mathcal{M}^2\rangle^2} \quad (33)$$

$$VAR\left\{\widehat{\Gamma_0}\right\} \geq \left(\frac{\Gamma_0 \ln(10)}{10}\right)^2 \frac{\sigma^2}{S}\frac{\langle \mathcal{M}^4\rangle}{\langle \mathcal{M}^4\rangle - \langle \mathcal{M}^2\rangle^2} \quad (34)$$

$$VAR\left\{\widehat{\sigma_N}\right\} \geq \left(\frac{\sigma_N^3}{20\log_{10}(e)}\right)^2 \frac{\sigma^2}{S}\frac{4}{\langle \mathcal{M}^4\rangle - \langle \mathcal{M}^2\rangle^2} \quad (35)$$

$$VAR\left\{\widehat{\theta_0}\right\} \geq \frac{\sigma^2}{S}\left(\frac{\sigma_N^2}{10\log_{10}(e)}\right)^2 \frac{1}{\langle \mathcal{M}^2\rangle} \quad (36)$$

All of the bounds considered in this section can be reduced by maximizing the angular dispersion of the sensors, regardless of distances. This makes sense, given that in this subsection we are primarily attempting to determine the directionality parameters of the transmitter.

It is also instructive to compare (28) and (34), which are both bounds for the peak transmitted power. In the former case, the beam width was known and the path loss was unknown, hence the angular spread of the sensors was immaterial but the variance in sensor distances was crucial. In the latter case, the beam width was unknown and the path loss was known, hence the angular spread governed the bound rather than the spread in distances.

D. Bounds on the RF topography

The ultimate goal of estimating the source's location and transmission parameters is the creation of a 5.1D RF topography. In this subsection, we derive the CRLB for the estimated power that would be incident across the spatial region of interest, as a function of the spatial coordinates.

The CRLB on a function of multiple parameters $g(\mathbf{z})$ is given by [17, p.229]

$$VAR\left\{\widehat{g(\mathbf{z})}\right\} \geq \left(\nabla_{\mathbf{z}} g\right)^T \mathbf{J}^{-1}\nabla_{\mathbf{z}} g. \quad (37)$$

In particular, let $\widehat{g(\mathbf{z})}$ be the estimated mean power (in the log domain) that would be received at a point (x, y), at a distance and angle of (d, θ) with respect to the source. The actual mean power is given by

$$g(\mathbf{z}) = P_0 - \frac{b}{2}\left(\mathcal{M}\left(\theta-\theta_0\right)\right)^2 - n_p\overline{d}, \quad (38)$$

$$\overline{d} = 10\log_{10}\sqrt{\left(x-x_0\right)^2 + \left(y-y_0\right)^2}, \quad (39)$$

$$\theta = \arctan\left(\frac{y-y_0}{x-x_0}\right). \quad (40)$$

The equations for the partial derivatives $\frac{\partial g}{\partial z_i}$ are nearly identical to (16)–(21), with the exception that the subscripts "s" are removed, hence the equations are not repeated here. Using (37), the variance of the estimated power can be determined as a function of position, providing a measure of confidence for each point in the topography.

IV. Estimation Algorithms

In this section, we derive algorithms for estimating the parameters of $\mathbf{z} = [P_0, b, n_p, \theta_0, x_0, y_0]$, using only observations of the log-normal distributed received power at the S sensors. First, we derive an ML algorithm for estimating the parameters when the source antenna has a Gaussian radiation pattern, in which it is known that the shape is Gaussian but the beam width is unknown. The algorithm reduces the search space for $\mathbf{z}$ from six dimensions to three dimensions, but due to the nonlinearity of the $\mathcal{M}(\cdot)$ function, a closed form solution for x_0, y_0, and θ_0 cannot be obtained, hence a three dimensional search is unavoidable. (A nonlinear least squares approach was considered as an alternative to a grid search over these three parameters, but due to slow convergence of the resulting algorithm, the results are not discussed here.) Second, we derive an ML algorithm for estimating the parameters when the radiation pattern of the source antenna has an arbitrary but completely known shape, with an isotropic antenna as a special case. Third, we create a hybrid, approximate ML algorithm that combines the computational simplicity of an algorithm based on the isotropic assumption with the accuracy of the full ML estimate.

A. ML estimation of a Gaussian beam

The ML algorithm takes the generic form

$$\widehat{\mathbf{z}}_{ML} = \arg\ \max_{\mathbf{z}}\ \underbrace{\ln f(\mathbf{p}|\mathbf{z})}_{L}. \tag{41}$$

In this case, the ML cost function L is given by (12), and for simplicity $\mathbf{C} = \sigma^2\mathbf{I}$ in the remainder of this section. Typically, (41) is solved by setting its gradient to zero and solving the resulting set of equations. The gradient equations are given by

$$\frac{\partial L}{\partial z_i} = \sum_{s=1}^{S} (p_s - m_s)\frac{\partial m_s}{\partial z_i}, \tag{42}$$

with the partial derivatives of m_s given by (16)–(21). Substituting in for m_s and simplifying, the first three gradient equations are

$$\frac{\partial L}{\partial P_0} = \sum_{s=1}^{S}\left(p_s - \left[P_0 - \frac{b}{2}\mathcal{M}^2 - n_p\overline{d}_s\right]\right) \tag{43}$$

$$\frac{\partial L}{\partial b} = \frac{-1}{2}\sum_{s=1}^{S}\left(p_s - \left[P_0 - \frac{b}{2}\mathcal{M}^2 - n_p\overline{d}_s\right]\right)\mathcal{M}^2 \tag{44}$$

$$\frac{\partial L}{\partial n_p} = -\sum_{s=1}^{S}\left(p_s - \left[P_0 - \frac{b}{2}\mathcal{M}^2 - n_p\overline{d}_s\right]\right)\overline{d}_s. \tag{45}$$

The equations for x_0, y_0, and θ_0 have been omitted since they are highly nonlinear and as such, a grid search will ultimately be necessary in order to solve them. Fortunately, P_0, b, and n_p are linearly dependent on the other three quantities, and we now proceed to solve for them in terms of x_0, y_0, and θ_0.

Setting (43)–(45) to zero, dividing by S, and using the "sample average" notation yields

$$\langle p_s\rangle - P_0 + \frac{b}{2}\langle\mathcal{M}^2\rangle + n_p\langle\overline{d}_s\rangle = 0 \tag{46}$$

$$\langle p_s\mathcal{M}^2\rangle - P_0\langle\mathcal{M}^2\rangle + \frac{b}{2}\langle\mathcal{M}^4\rangle + n_p\langle\overline{d}_s\mathcal{M}^2\rangle = 0 \tag{47}$$

$$\langle p_s\overline{d}_s\rangle - P_0\langle\overline{d}_s\rangle + \frac{b}{2}\langle\mathcal{M}^2\overline{d}_s\rangle + n_p\left\langle\overline{d}_s^2\right\rangle = 0. \tag{48}$$

Equations (46)–(48) can simultaneously be solved for P_0, b, and n_p by casting them into matrix form and using a 3×3 matrix inverse,

$$\begin{bmatrix}\widehat{P_0}\\ \widehat{b}\\ \widehat{n_p}\end{bmatrix} = \begin{bmatrix}1 & \frac{-1}{2}\langle\mathcal{M}^2\rangle & -\langle\overline{d}_s\rangle\\ \langle\mathcal{M}^2\rangle & \frac{-1}{2}\langle\mathcal{M}^4\rangle & -\langle\overline{d}_s\mathcal{M}^2\rangle\\ \langle\overline{d}_s\rangle & \frac{-1}{2}\langle\mathcal{M}^2\overline{d}_s\rangle & -\left\langle\overline{d}_s^2\right\rangle\end{bmatrix}^{-1}\begin{bmatrix}\langle p_s\rangle\\ \langle p_s\mathcal{M}^2\rangle\\ \langle p_s\overline{d}_s\rangle\end{bmatrix} \tag{49}$$

If one or more of P_0, b, or n_p is already known, then the relevant row(s) and column(s) of (49) should be omitted.

In summary, the ML estimation of the six unknowns (or a subset thereof) is accomplished by:

1) Pick a point in x_0, y_0, θ_0 space, chosen from a 3D grid.
2) Solve (49) for the ML estimates of P_0, b, and n_p, assuming the current x_0, y_0, and θ_0 are correct.
3) Evaluate the ML cost for the six tentative parameter estimates, via (12).
4) Repeat steps (1)-(3) for all points in the 3D grid.
5) Choose the x_0, y_0, and θ_0 from the grid that maximize (12), and retain the corresponding P_0, b, and n_p from (49).

The performance of this algorithm will be compared to the CRLB in Section V.

B. ML estimation of arbitrary, known radiation patterns

For the general class of radiation patterns of (3), the mean power in the dB domain is

$$m_s = 10\log_{10}\left(|G_g(\theta_s)|^2\right) - n_p\overline{d}_s, \tag{50}$$

$$= P_0 - \gamma\left(\mathcal{M}(\theta_s - \theta_0)\right) - n_p\overline{d}_s. \tag{51}$$

Note that the shape of the radiation pattern is considered completely known, i.e. there is no width-scaling parameter analogous to σ_N in this subsection. Equation (42) still applies, hence

$$\frac{\partial L}{\partial P_0} = \sum_{s=1}^{S}\left(p_s - \left[P_0 - \gamma\left(\mathcal{M}(\theta_s-\theta_0)\right) - n_p\overline{d}_s\right]\right) \tag{52}$$

$$\frac{\partial L}{\partial n_p} = -\sum_{s=1}^{S}\left(p_s - \left[P_0 - \gamma\left(\mathcal{M}(\theta_s-\theta_0)\right) - n_p\overline{d}_s\right]\right)\overline{d}_s. \tag{53}$$

Setting (52) and (53) to zero, dividing by S, and using the "sample average" notation yields

$$\langle p_s\rangle - P_0 + \langle\gamma\left(\mathcal{M}(\theta_s-\theta_0)\right)\rangle + n_p\langle\overline{d}_s\rangle = 0 \tag{54}$$

$$\langle p_s\overline{d}_s\rangle - P_0\langle\overline{d}_s\rangle + \langle\gamma\left(\mathcal{M}(\theta_s-\theta_0)\right)\overline{d}_s\rangle + n_p\left\langle\overline{d}_s^2\right\rangle = 0. \tag{55}$$

These two equations can be solved in matrix-vector form, as in (49). Since a 2×2 matrix can be inverted in closed form, the tentative estimates are

$$\widehat{P_0} = \frac{\left\langle\overline{d}_s^2\right\rangle\langle p_s\rangle - \langle\overline{d}_s\rangle\langle\overline{d}_s p_s\rangle + \left\langle\overline{d}_s^2\right\rangle\langle\gamma_s\rangle - \langle\overline{d}_s\rangle\langle\overline{d}_s\gamma_s\rangle}{\left\langle\overline{d}_s^2\right\rangle - \langle\overline{d}_s\rangle^2} \tag{56}$$

$$\widehat{n_p} = \frac{\left\langle \overline{d}_s \right\rangle \langle p_s \rangle - \left\langle \overline{d}_s p_s \right\rangle + \left\langle \overline{d}_s \right\rangle \langle \gamma_s \rangle - \left\langle \overline{d}_s \gamma_s \right\rangle}{\left\langle \overline{d}_s^2 \right\rangle - \left\langle \overline{d}_s \right\rangle^2}. \tag{57}$$

where γ_s is shorthand for $\gamma\left(\mathcal{M}\left(\theta_s - \theta_0\right)\right)$. This leads to a generic ML estimation algorithm for the case when the gain pattern is arbitrary but known numerically:

1) Pick a point in x_0, y_0, θ_0 space, chosen from a 3D grid.
2) Solve (56) and (57) for the ML estimates of P_0 and n_p, assuming the current x_0, y_0, and θ_0 are correct.
3) Evaluate the ML cost for the five tentative parameter estimates, via (12).
4) Repeat steps (1)-(3) for all points in the 3D grid.
5) Choose the x_0, y_0, and θ_0 from the grid that maximize (12), and retain the corresponding P_0 and n_p from (56) and (57).

This generic algorithm includes the special case of an omni-directional antenna, for which $\gamma(\cdot) = 0$. In that case, θ_0 is omitted, and the grid search is only over 2D rather than 3D.

C. Approximate ML estimation

The main drawback of the ML estimator of Section IV-A is that it requires a 3D search over x_0, y_0, and θ_0, which is computationally cumbersome. In this section, we form a hybrid algorithm that uses a heuristic to reduce the search space to 2D, but is ML over the 2D search space.

A directional antenna will broadcast most of its power in the direction in which it points. Consequently, a localization algorithm that ignores the directionality of the source (i.e., one that makes the omni-directional assumption) will tend estimate the source location to be directly in front of the true source location, i.e. in the direction pointed to by the true θ_0. (For example, the reader may jump ahead to Fig. 8.) This fact can be used to roughly estimate the transmitter orientation. Specifically, the approximate ML algorithm is:

0) Estimate the location of the source assuming omni-directional transmission, either by the algorithm in Section IV-B, or by an algorithm that does not estimate path loss and transmitted power. Call this estimate (x_{omni}, y_{omni}).
1) Pick a point in x_0, y_0 space, chosen from a 2D grid. Choose θ_0 to point from (x_0, y_0) to (x_{omni}, y_{omni}).
2) Solve (49) for the ML estimates of P_0, b, and n_p, assuming the current x_0, y_0, and θ_0 are correct.
3) Evaluate the ML cost for the six tentative parameter estimates, via (12).
4) Repeat steps (1)-(3) for all points in the 2D grid.
5) Choose the x_0 and y_0 from the grid that maximize (12), and retain the corresponding θ_0, P_0, b, and n_p.
6) (optional) In the vicinity of this solution, perform a local ML search over x_0, y_0, and θ_0 to refine their estimates.

Step (0) adds very little complexity, since the search space has few parameters compared to the full solution (no orientation or beam width). The authors have observed that if step (6) is omitted, x_0 and y_0 are generally almost identical to the ML solution, and θ_0 is sometimes (but rarely) off by up to 10^o. (These observations were made using the Gaussian radiation pattern.) If step (6) is included with a small search space, the accuracy of the full ML solution can be obtained with very low complexity.

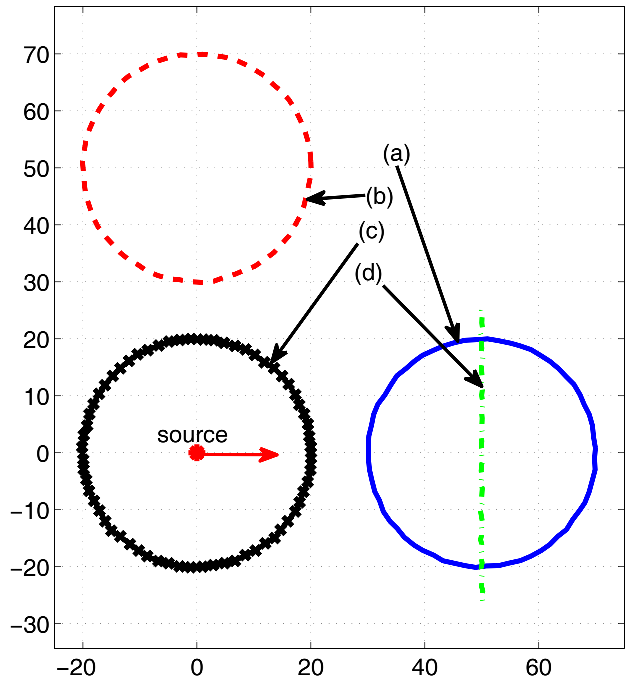

Fig. 2. The four sensor geometries used in Section V. The $*$ is the transmitter, which is oriented to transmit in the direction shown by the arrows. There are $S = 64$ sensors, regularly spaced along each of the four depicted geometries (in turn). Geometries (a), (c), and (d) obey the assumptions made in Section III-B.

V. Simulations and Numerical Evaluation

In this section, we first numerically evaluate the CRLB from Section III-A for four notional sensor geometries, in order to gain insight as to what type of sensor geometry leads to a good estimate of each parameter. Second, we test the three estimation algorithms of Section IV using a randomly placed array of a large number of sensors, including an evaluation of the bias and variance of the parameter estimates and an evaluation of how well each algorithm predicts the region in which the spectrum is available for use by a secondary user.

Unless otherwise specified, the true values of the unknown parameters are $(x_0, y_0) = (0, 0)$, $\theta_0 = 0$, and $n_p = 3$. The noise standard deviation σ is allowed to range from 4 dB to 12 dB, and where it is not considered an independent variable, it will be set to 5 dB. The directional antenna has beam half-width $\sigma_N = \pi/4$, and the peak transmit power is $P_0 = 20$ dBm at a reference distance of $d_0 = 1$ m.

Experiment 1 consists of Figs. 2 to 7 and Table I. The four sensor geometries shown in Fig. 2 are not quite perfect circles or lines; small displacements were added, since in some cases a perfect circle or line causes a singularity in the FIM. Adding small displacements (which also adds to the realism of the simulation) greatly enhances the numerical conditioning of the FIM. These displacements were Gaussian distributed with a standard deviation of 10 cm in each coordinate. Table I shows the relevant statistics of these four geometries.

Figs. 3 to 7 show the square root of the CRLB (i.e. the Root Mean Squared Error (RMSE)) on unbiased parameter estimates for the case where all 6 parameters are unknown.

TABLE I
STATISTICS OF THE FOUR SENSOR GEOMETRIES SHOWN IN FIG. 2.

Statistic	(a)	(b)	(c)	(d)
$\left\langle \overline{d}_s^2 \right\rangle$	290	290	169	295
$\left\langle \overline{d}_s^2 \right\rangle - \left\langle \overline{d}_s \right\rangle^2$	1.57	1.57	0.0004	0.026
$\left\langle (\theta_s - \theta_0)\, \overline{d}_s \right\rangle$	0.004	26.7	0.008	0.004
$\langle \theta_s - \theta_0 \rangle$	0.0002	1.57	0.0006	0.0003
$\langle \theta_s^2 \rangle - \langle \theta_s \rangle^2$	0.084	0.084	3.29	0.083

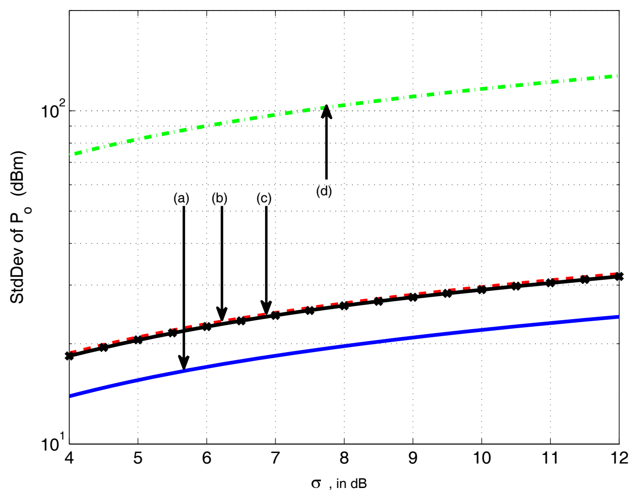

Fig. 3. The CRLB on P_0, for the four sensor geometries shown in Fig. 2.

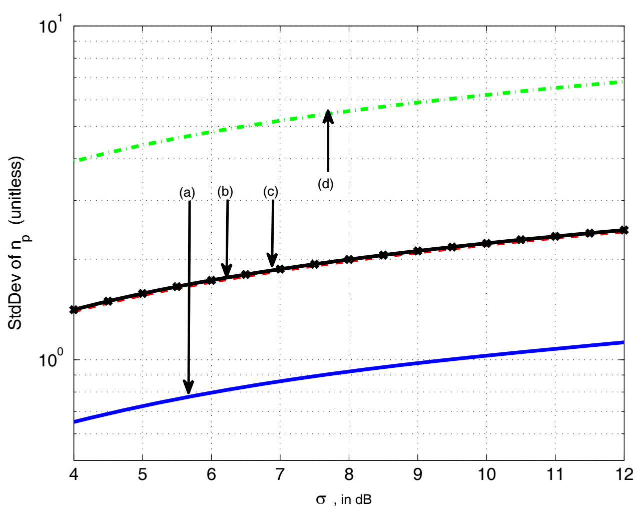

Fig. 4. The CRLB on n_p, for the four sensor geometries shown in Fig. 2.

In each geometry, $S = 64$ sensors were employed, regularly spaced along each circle or line. In general, the relative rankings of the different geometries do not change for similar experiments with fewer unknown parameters, but the bounds would all decrease. Geometry (c) is clearly the best for estimating the antenna location, orientation, and beam width, whereas geometry (a) is best for estimating power and path loss. In the case of known location and beam width (not shown, due to figure count limitations), geometry (b) performs as well as geometry (a). These relative rankings can be

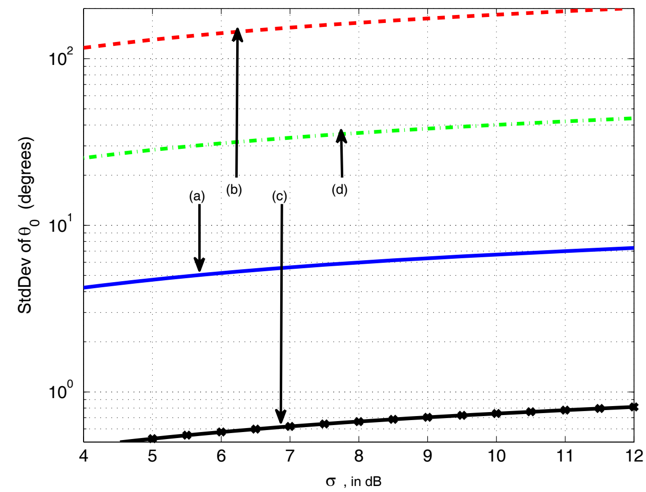

Fig. 5. The CRLB on θ_0, for the four sensor geometries shown in Fig. 2.

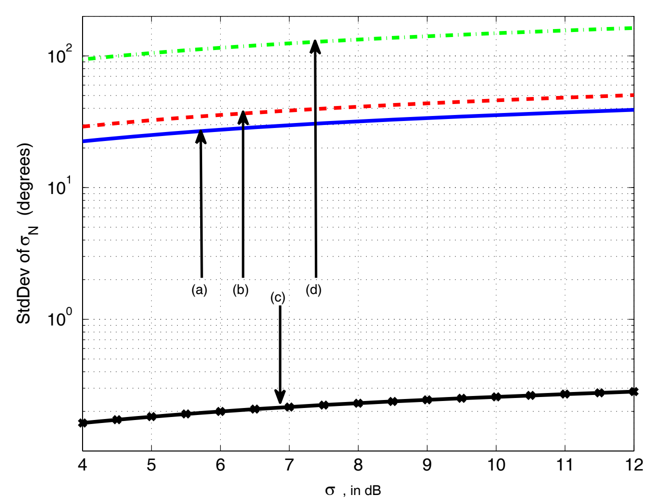

Fig. 6. The CRLB on σ_N, for the four sensor geometries shown in Fig. 2.

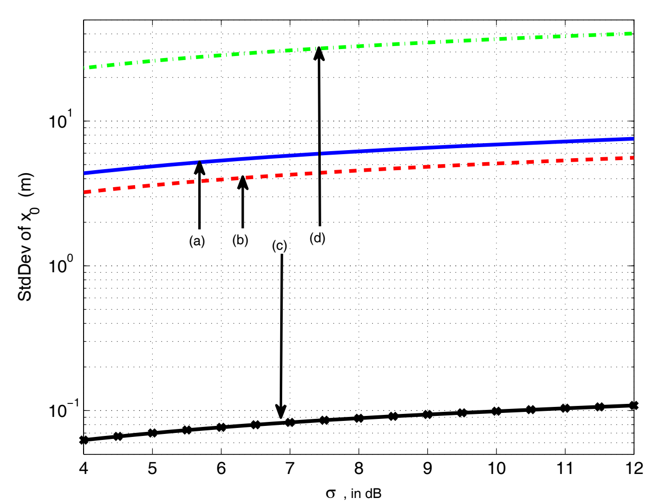

Fig. 7. The CRLB on x_0, for the four sensor geometries shown in Fig. 2.

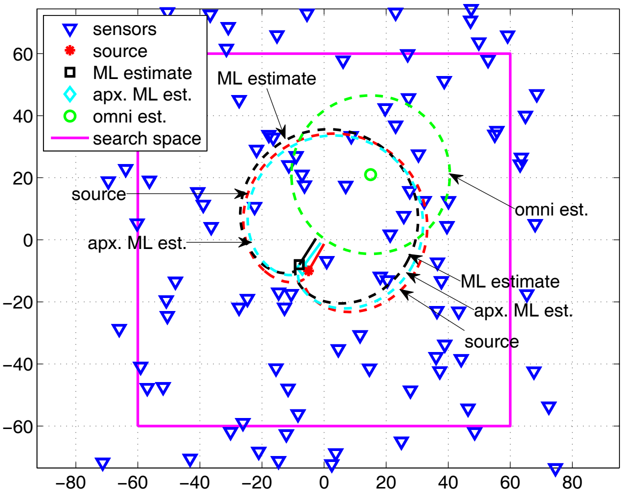

Fig. 8. Results of the three estimation algorithms discussed in Section IV. The contours indicate the true and estimated regions in which the received power is above a pre-set threshold, meaning that the spectrum is unavailable for use by a secondary user.

understood by considering the special case shown in (28), (29), and (30), which applies to (a), (c), and (d), although the resulting intuition appears to apply loosely to (b) as well. Geometries (a) and (b) have the largest distance variances, leading to good estimates of power and path loss; and (c) has the largest angular variance, leading to a good estimate of transmitter orientation. An optimal placement of sensors thus should have large variances in both angle and distance.

Experiment 2 consists of Fig. 8 (a sample result) and Table II (average results). Fig. 8 shows the results of the three estimation methods discussed in Section IV. These include ML estimation of all six unknowns, ML estimation that incorrectly assumes that the source is omni-directional with only four parameters to be estimated (P_0, n_p, x_0, and y_0), and approximate ML estimation that leverages the omni-directional estimate (without step (6)). $S = 100$ sensors were randomly distributed in a 150 m $\times$ 150 m area, and all other parameters were as above. The contours indicate the true and estimated regions in which the received power is above a threshold of -30 dBm (i.e. 50 dB below Γ_0), meaning that the spectrum is unavailable for use by a secondary user. Although the proposed ML estimator is not perfect, it does a fairly good job of estimating the spatial region in which spectrum is unavailable. In contrast, the incorrect omni-directional assumption leads to a poor estimate of spectrum unavailability, although it does partially overlap with the correct region. If the approximate ML estimator is used with step (6), it will produce the same solution as the ML estimator.

Table II shows the statistics of the ML estimates. The results were averaged over 1000 realizations of the additive noise. The geometry was as shown in Fig. 8, and all other parameters were as specified above. For each parameter, the standard deviation of the estimate dominated the bias and exceeded the square root of the CRLB. Thus, while the ML estimators cannot analytically be guaranteed to be unbiased, in practice the bias appears small compared to the estimator standard deviation. It is known that the ML estimator is

TABLE II
COMPARISON OF THE BIAS AND STANDARD DEVIATION OF ML PARAMETER ESTIMATES TO THE SQUARE ROOT OF THE CRLB AND THE RESOLUTION OF THE SEARCH SPACE.

Variable	value	avg est	bias	std dev	$\sqrt{\text{CRLB}}$	res.
x_0 (m)	-5	-5.76	-0.76	1.72	0.10	1.0
y_0 (m)	-10	-10.42	-0.42	1.81	0.17	1.0
θ_0 (deg)	60	59.82	-0.18	2.77	0.29	1.0
P_0 (dBm)	20	20.48	0.48	4.36	0.61	N/A
σ_N (deg)	45	44.69	-0.31	1.59	0.22	N/A
n_p (unitless)	3	3.02	0.02	0.25	0.03	N/A

asymptotically unbiased and efficient; although it appears that with six unknowns and 100 sensors, the ML estimator is not quite within the asymptotic regime.

Additional simulations, not included here due to space limitations, have shown that a modest amount of radiation pattern distortion does not adversely affect the proposed approach. The distortions considered include smearing out the beam pattern angularly by 10% to 25%, and adding a floor on the loss behind the antenna of -20 dB. This mimics the effects of scatterers close to and directly in front of the antenna, which may cause energy to fill in notches in the beam pattern. In the limit of wider amounts of blurring and higher floors (i.e. a very dense scattering environment immediately surrounding the transmitter), the effective radiation pattern becomes isotropic and the distinction between the proposed work and past work diminishes.

Now consider computational complexity. In our simulations, the numbers of grid points in the search space were $N_x = 121$, $N_y = 121$, and $N_\theta = 360$, and there were $S = 100$ sensors. All algorithms that assume directionality require $SN_xN_yN_\theta = 5.3 \times 10^8$ logs, divisions, and arctangents to compute angles and log-distances, which are inherent to the problem. The algorithm in Section IV-A requires an additional $7SN_xN_yN_\theta = 3.7 \times 10^9$ multiply-adds. Assuming evaluation of the $\gamma(\cdot)$ function requires 2 multiply-adds, the algorithm in Section IV-B uses $5SN_xN_yN_\theta = 2.6 \times 10^9$ multiply-adds. If this algorithm is used to localize an omni-directional source, then it only requires $3SN_xN_y = 4.4 \times 10^6$ multiply-adds. The fast algorithm in Section IV-C uses $10SN_xN_y = 1.5 \times 10^7$ multiply-adds, since it must perform omni-directional localization for initialization before performing directional localization.

On a 2.49 GHz desktop with a dual core processor, running Matlab release R2009a, the ML estimate used 765 s of CPU time, the approximate ML estimate used 5.1 s, and the omni-directional estimate used 1.4 s, in order to generate the results in Fig. 8.

VI. CONCLUSIONS

This paper derived performance bounds, an ML algorithm, and an approximate ML algorithm for estimation of a transmitter's location, orientation, beam width, power, and path loss exponent, using RSS measurements. As opposed to previous related work, this paper considered a directional transmitter. Power and path loss are best estimated when the distances from the source to the sensors have a large variance; whereas position, orientation, and beam width are best estimated when the the angular variance of the sensors is large with respect to the direction of transmission. The proposed parameter estimation algorithms can be used to improve decisions in a dynamic spectrum access system by indicating where the spectrum is available as a function of spatial coordinates, rather just spectral and temporal. This work forms the first step in our development of a 5.1D RF topography, which will assist cognitive network decision making.

REFERENCES

[1] R. W. Thomas, L. A. DaSilva, and A. B. Mackenzie, "Cognitive networks," in *Proc. IEEE DySPAN 2005*, Nov. 2005, pp. 352–360.

[2] P. Mähönen, M. Petrova, J. Riihijärvi, and M. Wellens, "Cognitive wireless networks: your network just became a teenager," in *Proc. IEEE INFOCOM 2006*, 2006.

[3] K. E. Nolan, P. D. Sutton, and L. E. Doyle, "A framework for implementing cognitive functionality," in *Proc. SDR Forum*, 2006.

[4] C. R. C. M. da Silva, W. C. Headley, J. D. Reed, and Y. Zhao, "The application of distributed spectrum sensing and available resource maps to cognitive radio systems," 2008.

[5] S. M. Mishra, A. Sahai, and R. W. Brodersen, "Cooperative sensing among cognitive radios," in *Proc. ICC 2006*, 2006, pp. 1658–1663.

[6] Y. Zhao, B. Le, and J. Reed, "Network Support: The Radio Environment Map," in *Cognitive Radio Technology*, 2nd edition, B. Fette, ed. Academic Press, 2008.

[7] W. Krenik and A. Batra, "Cognitive radio techniques for wide area networks," in *Proc. 42nd Design Automation Conference*, Anaheim, CA, June 2005.

[8] J. Zhu, S. Spain, T. Bhattacharya, and G. D. Durgin, "Performance of an indoor/outdoor RSS signature cellular handset location method in Manhattan," in *Proc. IEEE Int. Symp. Antennas and Propagation Society*, July 2006, pp. 3069–3072.

[9] D. Blatt and A. O. Hero, III, "Energy-based sensor network source localization via projection onto convex sets," *IEEE Trans. Signal Process.*, vol. 54, no. 9, pp. 3614–3619, Sep. 2006.

[10] H. Wang and P. Chu, "Voice source localization for automatic camera pointing system in video conferencing," in *Proc. IEEE Int. Conf. on Acoustics, Speech, and Signal Processing*, vol. 1, Munich, Germany, Apr. 1997, pp. 187–190.

[11] T. K. S. Stephen, "Source localization using wireless sensor networks," Master's thesis, Naval Postgraduate School, June 2006.

[12] G. Sun, J. Chen, W. Guo, and K. J. R. Liu, "Signal processing techniques in network-aided positioning," *IEEE Signal Process. Mag.*, vol. 22, pp. 12–23, July 2005.

[13] M. Rabbat and R. Nowak, "Decentralized source localization and tracking," in *Proc. Int. Conf. on Acoustics, Speech, and Signal Processing*, vol. 3, Montreal, Canada, May 2004, pp. 921–924.

[14] J. J. Caffery, Jr. and G. L. Stuber, "Overview of radiolocation in CDMA cellular systems," *IEEE Commun. Mag.*, vol. 36, no. 4, pp. 38–45, Apr. 1998.

[15] M. Kieffer and E. Walter, "Centralized and distributed source localization by a network of sensors using guaranteed set estimation," in *Proc. Int. Conf. Acoustics, Speech, & Signal Proc.*, vol. 4, Toulouse, France, May 2006, pp. 977–980.

[16] A. Catovic and Z. Sahinoglu, "The Cramér-Rao bounds of hybrid TOA/RSS and TDOA/RSS location estimation schemes," *IEEE Commun. Lett.*, vol. 8, no. 10, pp. 626–628, Oct. 2004.

[17] L. L. Scharf, *Statistical Signal Processing*. Addison Wesley, 1991.

[18] A. J. Weiss, "On the accuracy of a cellular location system based on RSS measurements," *IEEE Trans. Veh. Technol.*, vol. 52, no. 6, pp. 1508–1518, Nov. 2003.

[19] N. Patwari, A. O. Hero, III, M. Perkins, N. S. Correal, and R. J. O'Dea, "Relative location estimation in wireless sensor networks," *IEEE Trans. Signal Process.*, vol. 51, no. 8, pp. 2137–2148, Aug. 2003.

[20] H. Koorapaty, "Barankin bounds for position estimation using received signal strength measurements," in *Proc. IEEE Vehicular Technology Conf.*, vol. 5, Milan, Italy, May 2004, pp. 2686–2690.

[21] Y. Okumura, E. Ohmori, T. Kawano, and K. Fukuda, "Field strength and its variability in VHF and UHF land-mobile radio service," *Rev. Elec. Commun. Lab.*, vol. 16, pp. 9–10, 1968.

[22] T. S. Rappaport, *Wireless Communications: Principles and Practice*. Englewood Cliffs, NJ: Prentice-Hall, 1996.

Richard K. Martin received dual B.S. degrees (*summa cum laude*) in physics and electrical engineering from the University of Maryland, College Park in 1999, and the M.S. and Ph.D. degrees in electrical engineering from Cornell University, Ithaca, NY, in 2001 and 2004, respectively. Since August 2004, he has been an Assistant Professor at the Air Force Institute of Technology (AFIT), Dayton, OH. Dr. Martin has been elected "ECE Instructor of the Quarter" three times and "HKN Instructor of the Year" twice, by the AFIT students. His research interests include equalization for multicarrier and single-carrier cyclic-prefixed systems; blind, adaptive filters; sparse adaptive filters; navigation and source localization; and cognitive radio. He has authored eighteen journal papers, thirty-seven conference papers, and four patents.

Maj Ryan W. Thomas is an Assistant Professor of Computer Engineering in the Department of Electrical and Computer Engineering, Air Force Institute of Technology, Wright-Patterson AFB, OH. He received his PhD in Computer Engineering from Virginia Polytechnic Institute and State University, Blacksburg, VA in 2007; M.S. in Computer Engineering from the Air Force Institute of Technology, Wright-Patterson AFB, OH in 2001; and his B.S. from Harvey Mudd College in Claremont, CA in 1999. He previously worked at the Air Force Research Laboratory, Sensors Directorate as a digital antenna array engineer. Maj Thomas's research focuses on the design, architecture and evaluation of cognitive networks, cognitive radios and software defined radios.